ADVANCED MATERIALS
www.advmat.de

www.MaterialsViews.com

Tuning the Bandgap of Exfoliated InSe Nanosheets by Quantum Confinement

Garry W. Mudd, Simon A. Svatek, Tianhang Ren, Amalia Patanè, Oleg Makarovsky, Laurence Eaves, Peter H. Beton, Zakhar D. Kovalyuk, George V. Lashkarev, Zakhar R. Kudrynskyi, and Alexandr I. Dmitriev*

The discovery of single-atomic layer graphene[1] has led to a surge of interest in other anisotropic crystals with strong in-plane bonds and weak, van der Waals-like, inter-layer coupling.[2] A variety of two-dimensional (2D) crystals with high crystalline quality and stable properties under ambient conditions have been investigated recently. These include layers of large band gap insulators[3] such as boron nitride[4] and oxides,[5] and materials with smaller band gaps such as transition metal dichalcogenides[6,7] (e.g., MoS_2, $MoSe_2$, WS_2) and III–VI compounds (e.g., GaS and GaSe).[8] Interest in these systems is motivated partly by the possibility of combining them with graphene to create 2D electronic devices, e.g., field effect transistors with high on-off switching ratios[9,10] and memory cells.[11] More importantly, material systems with strong radiative recombination, specific dielectric properties, a band gap that can be adjusted by changing the layer thickness could offer opportunities for innovative device architectures in nanoelectronics and optoelectronics.[5,12,13]

Here we report the successful exfoliation of thin layers of γ-rhombohedral InSe, which is a semiconductor with a direct band gap and anisotropic electronic properties.[14–22] We demonstrate strong quantum confinement effects in these flakes, which have thickness L down to a few nanometres. The flakes are optically active at room temperature, in the technologically important near-infrared spectral range between 1 and 0.8 μm, thus offering unique opportunities for planar device architectures and near-infrared optical sensing. In particular, we show that the near-band edge photoluminescence (PL) peak and absorption-induced photoconductivity undergo a strong blue-shift to higher photon energies with decreasing L, consistent with 2D quantum confinement of photo-excited carriers by atomically flat interfaces; we observe a quenching of the PL signal in the thinnest flakes (L < 6 nm), which points to a direct-to-indirect band gap crossover and contrasts with the indirect-to-direct band gap transition previously reported for transition metal dichalcogenides as the film thickness is decreased.[6,23,24] Also, we show that the quantum confinement energies for the direct exciton in these InSe nanoflakes are one order of magnitude larger than those reported in other III–VI compounds, such as GaSe.[25]

Our samples are prepared from bulk Bridgman-grown crystals of γ-rhombohedral InSe. As shown in **Figure 1**a, the primitive unit cell of γ-InSe has a lattice parameter c = 24.961 Å (along the c-axis) and contains three layers, each consisting of four closely-packed, covalently bonded, monoatomic sheets in the sequence Se-In-In-Se. Within each plane, atoms form hexagons with lattice parameter a = 4.002 Å. The cleaved facets of InSe layered crystals are atomically smooth and contain a low-density of surface states.[26–28] The layers interact by weak van der Waals forces, resulting in anisotropic mechanical properties. Thin flakes of InSe from about 1 to 10^3 μm^2 in size were prepared from as-grown InSe crystals by mechanical exfoliation with adhesive tape. They were then deposited on various substrates (silicon oxide/Si, glass or mica) and immersed in acetone to remove the tape residuals.

Figure 1 shows AFM (Figure 1b) and optical (Figure 1c) images, and height z-scans (insets of Figure 1d,e) of a typical thin exfoliated flake on a silicon oxide/Si substrate. InSe layers of different thickness L (down to ≈4 nm) and single monolayer steps (≈1 nm) were identified by AFM. Room temperature (T = 300 K) μPL maps and corresponding μPL spectra of representative flakes are shown in Figure 1d,e and **Figure 2**. The near-band edge PL peak is centred at around hv = 1.25 eV for as-grown bulk crystals and for L > 15 nm. With decreasing L, the PL emission exhibits a strong blue-shift to high photon energies up to 200 meV (Figure 2a and **Figure 3**a), consistent with planar quantum confinement of photo-excited carriers by the external surfaces of the flakes. Concurrently, when L decreases below ~10 nm, the PL intensity decreases by a factor of >10, which is significantly larger than that expected from a reduction in the amount of luminescent material (Figure 2a,b), and the full width at half maximum (W) of the PL emission broadens by a factor of 2 (Figure 3b). The Raman spectra of the InSe nanoflakes and bulk crystals reveal the characteristic Raman peaks expected for γ-rhombohedral InSe.[29] The Raman signal intensity falls as expected due to a reduction in L of the absorbing material (see Supporting Information), in contrast to the PL intensity, which decreases by a greater factor when L < 10 nm (Figure 2b).

G. W. Mudd, S. A. Svatek, T. H. Ren, Prof. A. Patanè, Dr. O. Makarovsky, Prof. L. Eaves, Prof. P. H. Beton
School of Physics and Astronomy
The University of Nottingham
Nottingham, NG7 2RD, UK
E-mail: amalia.patane@nottingham.ac.uk
Prof. Z. D. Kovalyuk, Prof. G. V. Lashkarev, Prof. Z. R. Kudrynskyi, Prof. A. I. Dmitriev
Institute for Problems of Materials Science
Ukrainian Academy of Sciences, Kiev, Ukraine

DOI: 10.1002/adma.201302616

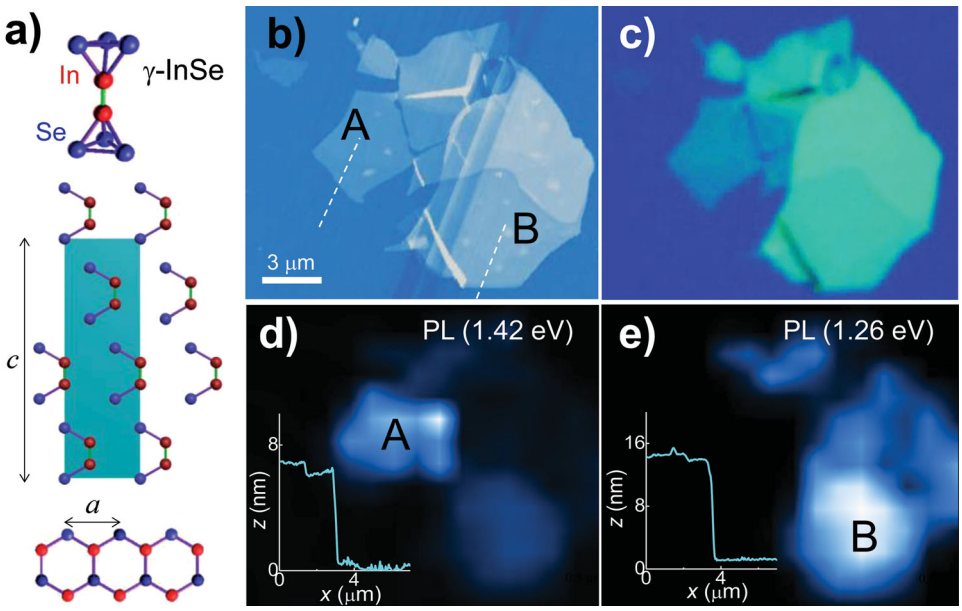

Figure 1. a) Crystal structure of γ-rhombohedral InSe. b) AFM and c) optical images of exfoliated InSe flakes on a silicon oxide/Si substrate. d,e) AFM *z*-profiles (insets) and confocal μPL maps at $T = 300$ K. The maps were obtained by plotting the μPL intensity at specific photon energies d) $h\nu = 1.42$ eV and e) 1.26 eV (laser power $P = 0.1$ mW and laser wavelength $\lambda = 633$ nm). The images show nanometer thick layers A and B with μPL emission centred at $h\nu = 1.42$ eV and 1.26 eV, respectively. The AFM *z*-profiles were obtained along the dotted lines shown in (b).

The PL emission of these exfoliated samples persists for several weeks when they are left in air, indicating their high chemical stability. Also, our photoconductivity measurements on planar diodes based on thin InSe flakes (down to 10 nm) show that the photoresponse of InSe is not impaired by the exfoliation procedure. In the absence of light, both the InSe as-grown crystals and flakes were found to be highly resistive with resistivity values of $\rho > 10$ Ωcm at room temperature, as measured by a standard two-probe method and under electric fields of up to ~1 kV cm^{-1}. As shown in **Figure 4**, the room temperature photocurrent spectrum for the thin InSe flake (continuous line, $L = 10$ nm) reveals an absorption edge at photon energies $h\nu \approx 1.4$ eV. The spectrum is blue-shifted by ~200 meV relative to the spectra of thicker flakes (dotted line, $L = 75$ nm) and of the as-grown InSe (dashed line), thus confirming strong 2D carrier confinement.

Figure 3a shows the results of PL and AFM measurements on more than 100 flakes, giving us the dependence of the band-to-band direct edge transition energy, E_{2D}, on the flake thickness L. We model this dependence using a square quantum well potential of infinite height, i.e.

$$E_{2D} = E_g - E_b + \pi^2\hbar^2/2L^2\mu_{//c} \quad (1)$$

where $E_g = 1.2635$ eV and $E_b = 0.015$ eV are the direct band gap energy and exciton binding energy in bulk InSe at $T = 300$ K, respectively,[30] $\mu_{//c} = (1/m^e_{//c} + 1/m^h_{//c})^{-1} = 0.054\, m_e$ is the exciton reduced mass, as derived from the measured values of the electron ($m^e_{//c} = 0.08\, m_e$)[18] and hole ($m^h_{//c} = 0.17\, m_e$)[19] masses for motion along the *c*-axis, and m_e is the electron mass in vacuum. As shown in Figure 3a, the calculated $E_{2D}(L)$ curve (continuous line) describes well the measured values of the PL peak energy. The scatter in the individual data points from the calculated curve indicate that the real confinement potential may differ from the hard wall potential assumed in our simple model. In particular, carriers can be confined within an InSe layer of effective thickness that is smaller than that measured by AFM due to a thin surface film into which the carrier wave functions do not penetrate. Such a film can originate from the native oxidised surface layer that forms in as-grown InSe as a result of the chemisorption of water and oxygen molecules on a low density of dangling bonds on the InSe surface.[17]

The thinnest InSe flakes identified by PL have a thickness $L \approx 6$ nm, which corresponds to a 7-monolayer InSe nanoflake and to a room temperature PL emission peaked at $E_{2D} = 1.44$ to 1.47 eV. Although thinner InSe flakes were measured by AFM, no PL signal was detected in these layers. In spite of variations from flake to flake, the quenching of the PL at small L (<6 nm) is always observed, see Figure 2a,b. We attribute the strong decrease of the PL signal in the very thin flakes to a direct-to-indirect band gap crossover analogous to that induced in bulk γ-InSe by hydrostatic pressure[19,20] or in InSe nanoparticles by quantum confinement.[31,32] For the case of InSe nanoparticles, the intensity of the PL emission is dependent on the nanoparticle size due to the combined effects of the carrier confinement along the *c*-axis (*z*-axis) and in the *xy*-plane.[31–33] Fluorescence is observed in small nanoparticles (<5 nm). Larger nanoparticles are non-fluorescent as confinement along the *c*-axis becomes a dominant effect, leading to a reversal in the direct and indirect optical transitions.[31,32] In our two-dimensional γ-InSe flakes, quantum confinement along the *c*-axis due to the small values of L acts to shift the conduction band (CB) minimum at the

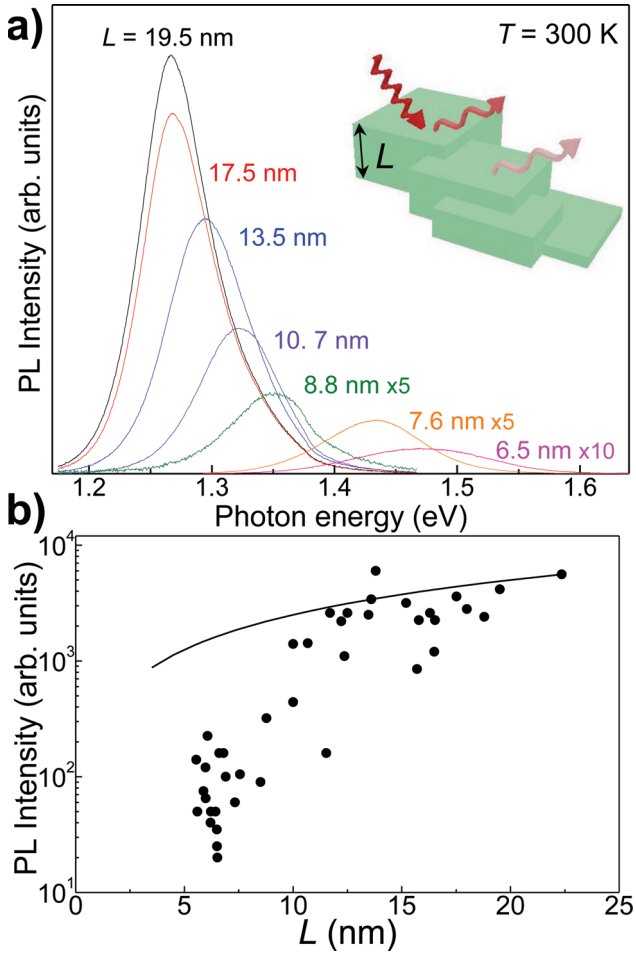

Figure 2. a) Typical μPL spectra of InSe layers at T = 300 K with peak energy strongly dependent on the layer thickness L (P = 0.1 mW and λ = 633 nm). The inset schetches the PL emission from flakes of different thickness L. b) L-dependence of the peak intensity of the μPL emission. The line describes the decrease in PL intensity that would be expected from a reduction in the amount of luminescent material with decreasing L.

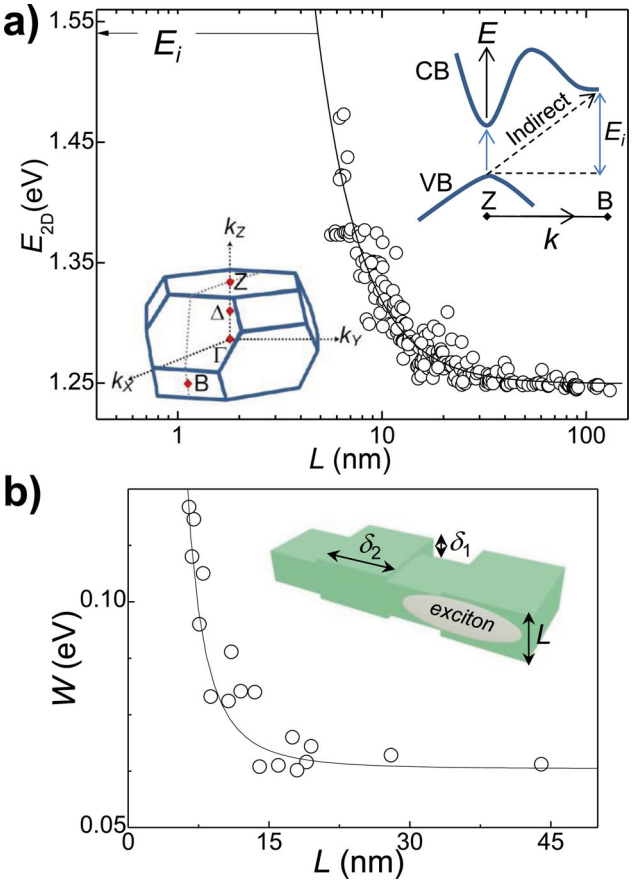

Figure 3. a) Measured dependence of the peak energy of the μPL emission, E_{2D}, on the thickness L of the InSe layer at T = 300 K. The continuous line shows the calculated dependence of the exciton recombination energy for a quantum well of width L. The horizontal arrow shows the energy E_i of the indirect gap between the valence band maximum at Z and the conduction band minimum at B (see insets for the sketch of the direct and indirect gap, the first Brillouin zone of bulk γ-InSe). b) Measured (symbols) and calculated (line) values of the PL full width at half maximum, W, versus L. The inset illustrates the roughness of the InSe quantum well layer.

Z-point of the Brillouin zone towards the upper B-minimum, the latter being less sensitive to quantum confinement owing to its larger electron effective mass, see inset in Figure 3a. The intersection between the calculated $E_{2D}(L)$ curve and the energy of the indirect band gap (E_i = 1.54 eV)[19,20] suggests that the direct-to-indirect gap crossover occurs at a critical layer thickness L = 5 nm (see Figure 3a), consistent with the quenching of the PL signal observed in our InSe nanosheets with L < 6 nm.

Our observations point towards a phenomenology which differs markedly from that reported for exfoliated MoS_2 and other transition metal dichalcogenides; in those materials, the intensity of the band-edge PL emission undergoes an abrupt increase when the flake thickness is reduced to a few monolayers owing to a crossover from an indirect-to-direct gap semiconductor.[6,23,24] Also, for transition metal dichalcogenides, the energy of the direct excitonic transition remains approximately constant (≈1.8 eV) as the thickness of the flake is varied. By contrast, for our InSe nanosheets the blue shifts of the PL emission energy are significant (up to about 200 meV), thus providing a means of tuning the absorption and emission of the flakes in the near-infrared spectral range not reported before for similar anisotropic crystals. The quantum confinement energies are also larger than those measured in other direct gaps III–VI compounds, such as GaSe, where decreasing L down to ~ 2 nm blue-shifts the PL emission by only 20 meV.[25] These observations reveal much stronger quantum confinement effects in InSe due to the smaller band gap (E_g = 1.2635 eV) and exciton reduced mass ($\mu_{//c}$ = 0.054 along the c-axis). This also causes a stronger sensitivity of the carrier recombination to the small roughness of the layers, as discussed below.

Our AFM images indicate that our exfoliated flakes are almost flat on the atomic scale with an average surface roughness of about one monolayer ($\delta_1 = c/3$ = 0.832 nm) along the c-axis (as determined by the standard deviation of the surface height distribution). However, the μPL studies show a systematic increase of the spectral linewidth of the PL emission with

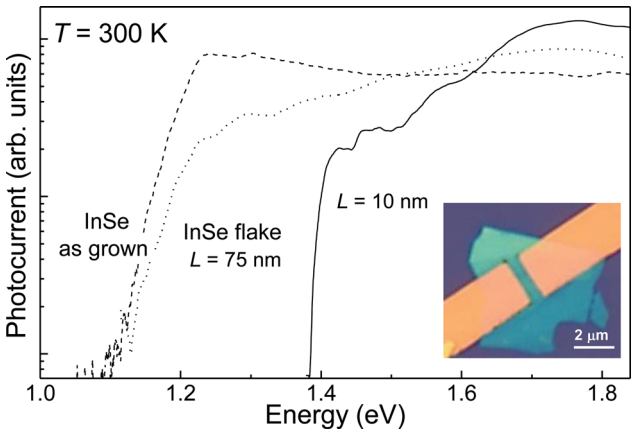

Figure 4. Photoconductivity spectra of two-terminal Ti/Au/InSe devices at $T = 300$ K ($P = 10^{-3}$ W cm^{-2}). The spectrum for the InSe flake with $L = 10$ nm (continuous line) is shifted to high energy relative to that for the as-grown InSe crystal (dashed line) and for the flake with $L = 75$ nm (dotted line). The inset is an optical image for the InSe flake with $L = 10$ nm.

decreasing L below 15 nm, see Figure 3b. To explain the optical broadening, we note that in quantum wells whose thickness is comparable with the exciton Bohr radius, a_{ex}, the PL emission depends on the uniformity of composition and abruptness of the interfaces. We quantify the spectral linewidth by using a simple statistical model of the exciton PL emission[34] that considers the roughness of the layers and the dependence of the exciton recombination energy E_{2D} on L. We assume that the two interfaces of the flake are comparable in quality, that the well width fluctuates by one monolayer (δ_1) around its mean value L and that the roughness consists of islands with thickness $L\pm\delta_1$, which have the same concentration and average lateral size δ_2. Hence we can describe the contribution of the interface roughness to the linewidth (full width at half maximum) as

$$W_R = \frac{\sqrt{2.8}}{4}\frac{\delta_2}{a_{ex}}(\Delta^+ + \Delta^-) \quad (2)$$

where $\Delta^{\pm} = \delta_1(\partial E_{2D}/\partial L)_{L\pm\delta_1}$.[34,35] Our model assumes a constant contribution to the linewidth (64 meV) from electron-phonon scattering and other disorder-related broadening effects that we have assumed to be independent of L. The calculated value of W_R increases monotonically with decreasing L and reproduces the measured data if we take the typical scale of the roughness δ_2 to be comparable to the exciton Bohr radius, i.e. $\delta_2/a_{ex} = 1.4 \pm 0.6$, see Figure 3b. For $a_{ex} = 8.6$ nm, this gives $\delta_2 = 12 \pm 5$ nm.[36] The good agreement between the model and experiment provides evidence for the strong carrier quantization and for the role of even a small degree of interface roughness on the PL linewidth of thin InSe flakes ($L < 15$ nm).

In conclusion, we have shown that the energy position and linewidth of the excitonic recombination in mechanically exfoliated Bridgman-grown crystals of γ-rhombohedral InSe can be well reproduced using an effective mass model of the quasi-2D carriers confined by the surfaces of the flakes. The quantization effects observed in InSe are much stronger than those previously reported in other van der Waals crystals, e.g., MoS_2, are also qualitatively different as they lead to a crossover from a direct-to-indirect gap when the thickness of the layers is reduced to a few nanometers ($L \approx 5$ nm) compared to the indirect-to-direct crossover found in transition metal dichalcogenides. 2D InSe flakes offer several advantages compared to 0D InSe nanocrystals and other III–VIs: the nanoflakes emit at room temperature, the thickness of the flake can be used to tune the absorption and emission in the technologically mid-infrared spectral range between 1 and 0.8 μm, the flake morphology is compatible with 2D electrodes. Thus these results should stimulate not only theoretical and experimental studies of the band structure of InSe nanosheets in the regime of strong quantum confinement, but also the use of InSe in planar 2D device architectures and novel band structure engineered devices.

Experimental Section

The bulk InSe crystals were studied by X-ray diffraction (XRD) using a DRON-3 X-ray diffractometer in a monochromatic Cu-Kα radiation of wavelenght $\lambda = 1.5418$ Å. The XRD data revealed that the InSe crystals had γ-phase structure with lattice constants $a = 4.002$ Å and $c = 24.961$ Å. Images of the InSe flake topography were acquired by atomic force microscopy (AFM) in non-contact mode under ambient conditions. The experimental set-up for μPL and Raman measurements comprised a He–Ne laser ($\lambda = 633$ nm), an XY linear positioning stage, an optical confocal microscope system, a spectrometer with 150 and 1200 groves/mm gratings, equipped with a charge-coupled device and a liquid-nitrogen cooled (InGa)As array photodetector. The laser beam was focused to a diameter $d \approx 1$ μm using a 100× objective and the μPL spectra were measured at low power ($P < 0.1$ mW) to avoid lattice heating. For the photoconductivity studies, we fabricated two-terminal planar devices on silicon oxide/Si substrates. Metal electrodes (3 nm Ti/30 nm Au) of width $w = 2.4$ μm separated by a distance $s = 0.6$ μm were deposited by electron beam lithography on the thin InSe flakes. Light from a 250 W quartz halogen lamp, dispersed through a 0.25 m monochromator (bandwidth of ≈10 nm) and modulated with a mechanical chopper, was focused onto the diodes ($P \approx 10^{-3}$ W cm^{-2}). The photocurrent signal was measured using a standard lock-in amplification technique.

Supporting Information

Supporting Information is available from the Wiley Online Library or from the author.

Acknowledgements

This work was supported by the Engineering and Physical Sciences Research Council (EPSRC), the University of Nottingham and the Ukrainian Academy of Sciences.

Received: June 7, 2013
Revised: July 9, 2013
Published online: August 21, 2013

[1] K. S. Novoselov, A. K. Geim, S. V. Morozov, D. Jiang, Y. Zhang, S. V. Dubonos, I. V. Grigorieva, A. A. Firsov, *Science* **2004**, *306*, 666.
[2] A. D. Yoffe, *Ann. Rev. Mater. Sci.* **1973** , *3*, 147.
[3] K. S. Novoselov, D. Jiang, F. Schedin, T. J. Booth, V. V. Khotkevich, S. V. Morozov, A. K. Geim, *Proc. Natl. Acad. Sci. USA* **2005**, *102*, 10451.

[4] C. R. Dean, A. F. Young, I. Meric, C. Lee, L. Wang, S. Sorgenfrei, K. Watanabe, T. Taniguchi, P. Kim, K. L. Shepard, J. Hone, *Nat. Nanotechnol.* **2010**, *5*, 722.
[5] M. Osada, T. Sasaki, *Adv. Mater.* **2012**, *24*, 210.
[6] K. F. Mak, C. Lee, J. Hone, J. Shan, T. F. Heinz, *Phys. Rev. Lett.* **2010**, *105*, 136805.
[7] S. Tongay, J. Zhou, C. Ataca, K. Lo, T. S. Matthews, J. Li, J. C. Grossman, J. Wu, *Nano Lett.* **2012**, *12*, 5576.
[8] D. J. Late, B. Liu, H. S. S. R. Matte, C. N. R. Rao, V. P. Dravid, *Adv. Func. Mater.* **2012**, *22*, 1894.
[9] L. Britnell, R. V. Gorbachev, R. Jalil, B. D. Belle, F. Schedin, A. Mishchenko, T. Georgiou, M. I. Katsnelson, L. Eaves, S. V. Morozov, N. M. R. Peres, J. Leist, A. K. Geim, K. S. Novoselov, L. A. Ponomarenko, *Science* **2012**, *335*, 947.
[10] T. Georgiou, R. Jalil, B. D. Belle, L. Britnell, R. V. Gorbachev, S. V. Morozov, Y.-J. Kim, A. Gholinia, S. J. Haigh, O. Makarovsky, L. Eaves, L. A. Ponomarenko, A. K. Geim, K. S. Novoselov, A. Mishchenko, *Nat. Nanotechnol.* **2013**, *8*, 100.
[11] S. Bertolazzi, D. Krasnozhon, A. Kis, *ACS Nano* **2013**, *7*, 3246.
[12] Q. H. Wang, K. Kalantar-Zadeh, A. Kis, J. N. Coleman, M. S. Strano, *Nat. Nanotechnol.* **2012**, *7*, 699.
[13] H. S. Lee, S. Min, Y. Chang, M. K. Park, T. Nam, H. Kim, J. H. Kim, S. Ryu, S. Im, *Nano Lett.* **2012**, *12*, 3695.
[14] J. Camassel, P. Merle, H. Mathieu, A. Chevy, *Phys. Rev. B* **1978**, *17*, 4718.
[15] M. Millot, J. M. Broto, S. George, J. Gonzalez, A. Segura, *Phys. Rev. B* **2010**, *81*, 205211.
[16] A. R. Goni, A. Cantarero, U. Schwarz, K. Syassen, A. Chevy, *Phys. Rev. B* **1992**, *45*, 4221.
[17] A. I. Dmitriev, V. V. Vishnjak, G. V. Lashkarev, V. L. Karbovskyi, Z. D. Kovaljuk, A. P. Bahtinov, *Phys. Sol. State* **2011**, *53*, 622.
[18] E. Kress-Rogers, R. J. Nicholas, J. C. Portal, A. Chevy, *Sol. State Comm.* **1982**, *44*, 379.
[19] F. J. Manjón, A. Segura, V. Muñoz-Sanjosé, G. Tobías, P. Ordejón, E. Canadell, *Phys. Rev. B* **2004**, *70*, 125201.
[20] F. J. Manjón, D. Errandonea, A. Segura, A V. Muñoz, G. Tobías, P. Ordejón, E. Canadell, *Phys. Rev. B* **2001**, *63*, 125330.
[21] G. V. Lashkarev, A. I. Dmitriev, V. K. Kiselyev, V. K. Kononenko, E. M. Kuleshov, *Int. J. Infrared Milli.* **1995**, *16*, 775.
[22] B. Gorshunov, A. Volkov, A. K. Prokhorov, M. Kondrin, S. Demishev, G. V. Lashkarev, A. I. Dmitriev, Z. D. Kovalyuk, *Sol. State Comm.* **1998**, *105*, 433.
[23] A. Splendiani, L. Sun, Y. Zhang, T. Li, J. Kim, C.-Y. Chim, G. Galli, F. Wang, *Nano Lett.* **2010**, *10*, 1271.
[24] P. Tonndorf, R. Schmidt, P. Böttger, X. Zhang, J. Börner, A. Liebig, M. Albrecht, C. Kloc, O. Gordan, D. R. T. Zahn, S. M. de Vasconcellos, R. Bratschitsch, *Optical Express* **2013**, *21*, 4908.
[25] P. Hu, Z. Wen, L. Wang, P. Tan, K. Xiao, *ACS Nano* **2012**, *6*, 5988.
[26] A. I. Dmitriev, G. V. Lashkarev, Z. D. Kovalyuk, V. I. Lazorenko, A. N. Zuganov, P. S. Smertenko, *Sol. St. Comm.* **1990**, *75*, 465.
[27] A. P. Bakhtinov, Z. D. Kovalyuk, O. N. Sydor, V. N. Katerinchuk, O. S. Lytvyn, *Phys. Sol. State* **2007**, *49*, 1572.
[28] A. I. Dmitriev, V. M. Kaminskiy, G. V. Lashkarev, P. E. Butorin, Z. D. Kovalyuk, V. I. Ivanov, A. M. Balagurov, A. I. Beskrovnyy, *Phys. Sol. State* **2009**, *51*, 2342.
[29] Z. D. Kovalyuk, O. M. Sydor, O. A. Sydor, V. G. Tkachenko, I. M. Maksymchuk, V. Iv. Dubinko, P. M. Ostapchuk, *J. Mat. Sci. Eng. A* **2012**, *2*(7), 537.
[30] O. Madelung, *Semiconductor: Data Handbook*, Springer, London **2003**, Ch. 23, p. 586.
[31] S. Yang, D. F. Kelley, *J. Phys. Chem. B* **2005**, *109*, 12701.
[32] S. Yang, D. F. Kelley, *J. Phys. Chem. B* **2006**, *110*, 13430.
[33] M. O. D. Camara, A. Mauger, I. Devos, *Phys. Rev. B* **2002**, *65*, 125206.
[34] J. Singh, K. K. Bajaj, S. Chaudhuri, *Appl. Phys. Lett.* **1984**, *44*, 805.
[35] A. Patanè, A. Polimeni, M. Capizzi, F. Martelli, *Phys. Rev. B* **1995**, *52*, 2784.
[36] We estimate the exciton radius using a bulk hydrogenic model, i.e. $a_{ex} = e^2/2\varepsilon_0\varepsilon E_b$. Here, $E_b = 0.015$ eV is the exciton binding energy and $\varepsilon = 7$ is the relative dynamic dielectric constant of γ-InSe.